NASA Technical Memorandum 85898

NASA-TM-85898 19840014260

Application of a Fractional-Step Method to Incompressible Navier-Stokes Equation

J. Kim and P. Moin

March 1984

NASA
National Aeronautics and
Space Administration

```
53      3      3 51*52
                                   CC028: INVALID COMMAND--PROCEED
                                   CC028: INVALID COMMAND--PROCEED
   DISPLAY                         DX111: PREVIOUS OUTPUT COMPLETED
54     49      49 AU/KEMP, N. H.
55      2       2 51*54
56      1       1 RN/NASA-TM-85898
          DISPLAY 56/2/1
      84N22328*#   ISSUE 12   PAGE 1893   CATEGORY 64   RPT#: NASA-TM-85898
      A-9665 NAS 1.15:85898   84/03/00  35 PAGES   UNCLASSIFIED DOCUMENT
UTTL: Application of a fractional-step method to incompressible Navier-Stokes
      equation
AUTH: A/KIM, J.;  B/MOIN, P.
CORP: National Aeronautics and Space Administration. Ames Research Center,
      Moffett Field, Calif.     AVAIL.NTIS   SAP: HC A03/MF A01
MAJS: /*ERROR ANALYSIS/*INCOMPRESSIBLE FLOW/*KINETIC ENERGY/*NAVIER-STOKES
      EQUATION
MINS: / BOUNDARY VALUE PROBLEMS/ STEP FUNCTIONS/ THREE DIMENSIONAL FLOW/ TIME
      DEPENDENCE/ VELOCITY DISTRIBUTION/ VISCOSITY
ABA:  Author
ABS:  A numerical method for computing three dimensional, time dependent
      incompressible flows is presented. The method is based on a fractional
      step, or time-splitting, scheme in conjunction with the
      approximate-factorization technique. The use of velocity boundary
      conditions for the intermediate velocity field leads to inconsistent
      numerical solutions. Appropriate boundary conditions for the intermediate
      velocity field are derived and tested. Numerical solutions for flow inside
      a driven cavity and over a backward-facing step are presented and compared
      with experimenal data and other numerical results.

ENTER:
```

NASA Technical Memorandum 85898

Application of a Fractional-Step Method to Incompressible Navier-Stokes Equation

J. Kim
P. Moin, Ames Research Center, Moffett Field, California

National Aeronautics and
Space Administration

Ames Research Center
Moffett Field. California 94035

N84-22328#

Application of a Fractional-Step Method to Incompressible Navier-Stokes Equations

J. KIM AND P. MOIN

Computational Fluid Dynamics Branch

NASA Ames Research Center, Moffett Field, California 94035

Received ______________

Manuscript pages: 20

Figures: 10

Tables: 3

Proposed running head:

FRACTIONAL-STEP METHOD

Send proofs to:

J. Kim

MS 202A-1

NASA Ames Research Center

Moffett Field, CA 94035

ABSTRACT

A numerical method for computing three-dimensional, time-dependent incompressible flows is presented. The method is based on a fractional-step, or time-splitting, scheme in conjunction with the approximate-factorization technique. It is shown that the use of velocity boundary conditions for the intermediate velocity field can lead to inconsistent numerical solutions. Appropriate boundary conditions for the intermediate velocity field are derived and tested. Numerical solutions for flows inside a driven cavity and over a backward-facing step are presented and compared with experimental data and other numerical results.

1. INTRODUCTION

In this paper we present a numerical method for solving three-dimensional, time-dependent incompressible Navier-Stokes equations. The major difficulty in obtaining a time-accurate solution for an incompressible flow arises from the fact that the continuity equation does not contain the time-derivative explicitly. The constraint of mass conservation is achieved by an implicit coupling between the continuity equation and the pressure in the momentum equations. One can use an explicit time-advancement scheme which obtains the pressure at the current time-step such that the continuity equation at the next step is satisfied. However, for fully implicit or semi-implicit schemes, the aforementioned difficulty prevents the use of the conventional alternating-direction-implicit (ADI) scheme to advance in time as is the case for compressible flows. This difficulty can be avoided in two-dimensional cases by reformulating the problem in terms of the vorticity and stream-function. For three-dimensional problems, one can introduce an artificial compressibility into the continuity equation to include the required time-derivative for an ADI scheme. This is satisfactory, however, only for the steady-state solutions [1]. For unsteady problems, since the effect of the artificial compressibility has to be minimized, this approach produces a highly stiff system for numerical solutions [2].

The objective of the present work is to develop a numerical method for solving the incompressible Navier-Stokes equations satisfying the conservation of mass exactly (within machine round-off). It will be also required that the numerical scheme preserve the global conservation of momentum, kinetic energy, and circulation in the absence of time-differencing errors and viscosity. It can be shown that failure to preserve these conservation properties can lead to numerical instabilities [3]. In order to stabilize the calculations using methods that do not preserve these properties, artificial viscosity is often introduced either explicitly or implicitly by using dissipative finite-difference schemes, especially for high-Reynolds-number flows.

The method developed herein is based on a fractional-step method (e.g., [4,5]) in conjunction with the approximate-factorization technique [6,7]. The flow field is represented on a staggered grid [8]. The problem of concocting boundary conditions for the intermediate (split) velocity field is addressed and it is shown that the use of velocity boundary conditions can lead to inconsistent and erroneous results. Appropriate boundary conditions for the intermediate-velocity field are derived using a technique similar to that of LeVeque and Oliger [9]. The Poisson equation for the pressure correction is solved by a direct method based on trigonometric expansions. In this way the continuity equation is satisfied to machine accuracy at every time-step.

The numerical procedures used in the present method are described in Section 2. Section 3 provides a derivation of the boundary conditions for the intermediate-velocity field, and numerical results for two different flow geometries are presented in Section 4; a summary is given in Section 5.

2. NUMERICAL METHOD

In this section we present a variant of the fractional-step method used by Chorin [4] for time-advancement of the Navier-Stokes and continuity equations for incompressible viscous flows:

$$\frac{\partial u_i}{\partial t} + \frac{\partial}{\partial x_j} u_i u_j = -\frac{\partial p}{\partial x_i} + \frac{1}{Re} \frac{\partial}{\partial x_j} \frac{\partial}{\partial x_j} u_i \ , \tag{1}$$

$$\frac{\partial u_i}{\partial x_i} = 0 \ . \tag{2}$$

Here, all variables are nondimensionalized by a characteristic velocity and length scale, and Re is the Reynolds number.

The fractional step, or time-split method, is in general a method of approximation of the evolution equations based on decomposition of the operators they contain. In application of this method to the Navier-Stokes equations, one can interpret the role of pressure in the momentum equations as a projection operator which projects an arbitrary vector field into a divergence-free vector field. A two-step time-advancement scheme for Eqs. (1) and (2) can be written as follows:

$$\frac{\hat{u}_i - u_i^n}{\Delta t} = \frac{1}{2}(3H_i^n - H_i^{n-1}) + \frac{1}{2}\frac{1}{Re}\left(\frac{\delta^2}{\delta x_1^2} + \frac{\delta^2}{\delta x_2^2} + \frac{\delta^2}{\delta x_3^2}\right)(\hat{u}_i + u_i^n) \ , \tag{3}$$

$$\frac{u_i^{n+1} - \hat{u}_i}{\Delta t} = -G(\phi^{n+1}) \ , \tag{4}$$

with

$$D(u_i^{n+1}) = 0 \ , \tag{5}$$

where $H_i = -(\delta/\delta x_j)u_i u_j$ is the convective terms, ϕ is a scalar to be determined, $\delta/\delta x_i$ represents discrete finite difference operators, and G and D represent discrete gradient and divergence operators, respectively. We used the second-order-explicit Adams-Bashforth scheme for the convective terms and the second-order-implicit Crank-Nicolson for the viscous terms. Implicit treatment of the viscous terms eliminates the numerical viscous stability restriction. Equation (3) is a second-order-accurate approximation of Eq. (1) with $\partial p/\partial x_i$ excluded. By substituting Eq. (4) into (3), one can easily show that the overall accuracy of the splitting method is still second order. Note that ϕ is different from the original pressure: in fact, $p = \phi + (\Delta t/2Re)\nabla^2\phi$. All the spatial derivatives are approximated with second-order central differences on a staggered grid [8]. Figure 1 illustrates the staggered grid. With the staggered mesh, the momentum equations are evaluated at the velocity nodes, and the continuity equation is enforced for each cell. One important advantage of using the staggered mesh for incompressible flows is that ad hoc pressure boundary conditions are not required. Furthermore, it can be shown [10] that with this approximation of spatial derivatives and in the absence of time-differencing errors and viscosity, global conservations of momentum, kinetic energy, and circulation are preserved.

Equation (3) can be rewritten as

$$(1 - A_1 - A_2 - A_3)(\hat{u}_i - u_i^n) = \frac{\Delta t}{2}(3H_i^n - H_i^{n-1}) + 2(A_1 + A_2 + A_3)u_i^n \,, \qquad (6)$$

where $A_1 = (\Delta t/2Re)(\delta^2/\delta x_1^2)$, $A_2 = (\Delta t/2Re)(\delta^2/\delta x_2^2)$, $A_3 = (\Delta t/2Re)(\delta^2/\delta x_3^2)$. The left-hand side of Eq. (6) is then approximated as follows:

$$(1 - A_1)(1 - A_2)(1 - A_3)(\hat{u}_i - u_i^n) = \frac{\Delta t}{2}(3H_i^n - H_i^{n-1}) + 2(A_1 + A_2 + A_3)u_i^n \ . \qquad (7)$$

Equation (7) is an $O(\Delta t^3)$ approximation to Eq. (6). However, it requires inversions of tridiagonal matrices rather than inversion of a large sparse matrix, as in the case of Eq. (6). This results in a significant reduction in computing cost and memory.

Equations (4) and (5) can be solved as coupled system equations for u_i^{n+1} and ϕ^{n+1} with boundary conditions for u_i^{n+1}. Note that since ϕ^{n+1} is defined at the center of each cell, there is a sufficient number of equations for u_i^{n+1} and ϕ^{n+1} without the need for boundary condition for ϕ^{n+1}. Equations (4) and (5) can be combined to eliminate u_i^{n+1} and thus obtain a set of equations for ϕ^{n+1}. For the cells not adjacent to the boundaries, these equations take the form of the discrete Poisson equation,

$$\left(\frac{\delta^2}{\delta x_1^2} + \frac{\delta^2}{\delta x_2^2} + \frac{\delta^2}{\delta x_3^2}\right) \phi^{n+1}(i,j,k) = \frac{1}{\Delta t} D\hat{u} \equiv Q(i,j,k) \ , \qquad (8)$$

for $i = 2,3,\ldots,N_1 - 1$, $j = 2,3,\ldots,N_2 - 1$, $k = 2,3,\ldots,N_3 - 1$. For the cells adjacent to the boundaries, incorporation of the velocity boundary conditions yields a modified set of equations. For example, for the cells adjacent to the lower boundary ($j = 1$), we obtain

$$\left(\frac{\delta^2}{\delta x_1^2} + \frac{\delta^2}{\delta x_3^2}\right) \phi^{n+1}(i,1,k) + \frac{1}{x_2\left(\frac{3}{2}\right) - x_2\left(\frac{1}{2}\right)} \frac{\phi^{n+1}(i,2,k) - \phi^{n+1}(i,1,k)}{x_2(2) - x_2(1)}$$

$$= \frac{1}{\Delta t} D\hat{u} - \frac{1}{\Delta t} \frac{u_2^{n+1}\left(i, \frac{1}{2}, k\right) - \hat{u}_2\left(i, \frac{1}{2}, k\right)}{x_2\left(\frac{3}{2}\right) - x_2\left(\frac{1}{2}\right)} \equiv Q(i,1,k) \qquad (9)$$

for $i = 2,3,\ldots,N_1 - 1$, $k = 2,3,\ldots,N_3 - 1$. A solution to Eq. (8) and the corresponding boundary equations can be easily obtained using transform methods [11]. Let

$$\phi^{n+1}(i,j,k) = \sum_{\ell=0}^{N_1-1} \sum_{m=0}^{N_3-1} \tilde{\phi}(\ell,j,m)\cos\left[\frac{\pi\ell}{N_1}\left(i - \frac{1}{2}\right)\right]\cos\left[\frac{\pi m}{N_3}\left(k - \frac{1}{2}\right)\right] \tag{10}$$

for $i = 1,2,\ldots,N_1$, $j = 1,2,\ldots,N_2$, $k = 1,2,\ldots,N_3$. Here we have assumed that uniform mesh spacings are used in the streamwise and spanwise directions (x_1 and x_3). If nonuniformly spaced mesh points are used in these directions, multigrid methods appear to be the best alternative to the transform method used here. Substituting Eq. (10) and the corresponding expansion for Q into (8) and (9) and using the orthogonality property of cosines, we obtain

$$\frac{\delta^2\tilde{\phi}}{\delta x_2^2} - k'_\ell\tilde{\phi} - k'_m\tilde{\phi} = \tilde{Q}(\ell,j,m) , \tag{11}$$

where $k'_\ell = 2[1 - \cos(\pi\ell/N_1)]/\Delta x_1^2$ and $k'_m = 2[1 - \cos(\pi m/N_3)]/\Delta x_3^2$ are the modified wave numbers. For each set of wave numbers, the above tridiagonal system of equations can be easily inverted, and ϕ^{n+1} is obtained from Eq. (10). The final velocity field u_i^{n+1} is then obtained from

$$u_i^{n+1} = \hat{u}_i - \Delta t G(\phi^{n+1}) \tag{12}$$

3. BOUNDARY CONDITIONS

Boundary conditions for the intermediate velocity fields in time-splitting methods are generally a source of ambiguity. At each complete time-step, only the boundary conditions for the velocity field are given and those of the intermediate velocity field are unknown. We will show in this section that except when the boundary conditions for the intermediate velocity field are chosen to be consistent with the governing equations, the solution may suffer from appreciable numerical errors. In the present work, we derive the appropriate boundary conditions for the intermediate velocity field using a method suggested by LeVeque and Oliger [9].

To construct the proper boundary conditions for $\hat{u}_i$, we regard $\hat{u}_i$ as an approximation to $u_i^*(\underline{x},t_{n+1})$ where the continuous function $u_i^*(\underline{x},t)$ satisfies

$$\left.\begin{aligned} \frac{\partial u_i^*}{\partial t} &= H_i^* + \frac{1}{Re}\frac{\partial}{\partial x_j}\frac{\partial}{\partial x_j}u_i^* \\ u_i^*(\underline{x},t_n) &= u_i(\underline{x},t_n) \ . \end{aligned}\right\} \tag{13}$$

Hence

$$\begin{aligned} \hat{u}_i &\simeq u_i^*(\underline{x},t_n + \Delta t) \\ &= u_i^*(\underline{x},t_n) + \Delta t\,\frac{\partial u_i^*}{\partial t} + \frac{1}{2}\Delta t^2\,\frac{\partial^2 u_i^*}{\partial t^2} + \ldots \qquad (14) \\ &= u_i^*(\underline{x},t_n) + \Delta t\left(H_i^* + \frac{1}{Re}\nabla^2 u_i^*\right) + \frac{1}{2}\Delta t^2\,\frac{\partial}{\partial t}\left(H_i^* + \frac{1}{Re}\nabla^2 u_i^*\right) + \ldots \ . \end{aligned}$$

Since $u_i^*(\underline{x},t_n) = u_i(\underline{x},t_n)$,

$$\begin{aligned} \hat{u}_i &= u_i(\underline{x},t_n) + \Delta t\left(H_i + \frac{1}{Re}\nabla^2 u_i\right) + \frac{1}{2}\Delta t^2\,\frac{\partial}{\partial t}\left(H_i + \frac{1}{Re}\nabla^2 u_i\right) + \ldots \\ &= u_i(\underline{x},t_n) + \Delta t\left(\frac{\partial u_i}{\partial t} + \frac{\partial p}{\partial x_i}\right) + \frac{1}{2}\Delta t^2\left(\frac{\partial^2 u_i}{\partial t^2} + \frac{\partial}{\partial t}\frac{\partial}{\partial x_i}p\right) + \ldots \qquad (15) \\ &= u_i(\underline{x},t_{n+1}) + \Delta t\,\frac{\partial p}{\partial x_i} + O(\Delta t^2) \ . \end{aligned}$$

By keeping the first two terms, we have boundary conditions accurate to $O(\Delta t^2)$. Since $p = \phi + O(\Delta t/Re)$, we can in fact use $\hat{u}_i = u_i^{n+1} + \Delta t \frac{\partial \phi^n}{\partial x_i}$ with the same accuracy, thus avoiding the computation of pressure explicitly.

These boundary conditions are tested in computing the following two-dimensional unsteady flow which is a solution to the Navier-Stokes and continuity equations [12,13]:

$$\left.\begin{aligned} u_1(x_1,x_2,t) &= -\cos x_1 \sin x_2 \, e^{-2t} \\ u_2(x_1,x_2,t) &= \sin x_1 \cos x_2 \, e^{-2t} \\ p(x_1,x_2,t) &= -\frac{1}{4}(\cos 2x_1 + \cos 2x_2)e^{-4t} . \end{aligned}\right\} \quad (16)$$

The maximum difference between the exact and numerical solutions from four different runs are listed in Table I. The superiority of the results using boundary conditions (15) over the results using the velocity boundary condition, $\hat{u}_i = u_i^{n+1}$, is clearly evident. In fact, the error for the latter case increases when the mesh is refined. This indicates that the fractional-step method with the latter boundary condition is an inconsistent scheme. To determine the overall accuracy of the scheme using the boundary condition (15), three calculations are performed with three different mesh sizes but keeping the Courant number constant. The variation of the maximum error with mesh refinement is plotted in Fig. 2; it shows that the scheme is indeed second-order accurate.

4. NUMERICAL EXAMPLES

In this section we present numerical results obtained from applications of the aforementioned numerical method to two laminar flow problems.

Both problems have been used widely as standard test cases for evaluating the stability and accuracy of numerical methods for incompressible flow problems.

4.1 Flow in a Driven Cavity

Figure 3 shows the geometry and the boundary conditions for the flow in a driven cavity together with the appropriate nomenclature. Flow is driven by the upper wall, and several standing vortices exist inside the cavity whose characteristics are functions of Reynolds numbers. Figures 4 and 5 show the computed results of streamlines, contours of constant vorticity, and velocity vectors for several Reynolds numbers. The purpose of the velocity-vector figures is to show the corner eddies, which are too weak to be displayed clearly by the streamlines. They are drawn parallel to the flow direction at each mesh point. At $Re = 1$, this flow is almost symmetric with respect to the centerline, and two corner eddies are visible. As Reynolds number increases, the center of the main vortex moves toward the downstream corner before it returns toward the center at higher Reynolds number. In the Reynolds number range, 1000-2000, the third corner eddy is formed at the upper left corner. At $Re = 5000$, a tertiary corner eddy is visible. In Fig. 6, the velocity at the middle of the cavity for $Re = 400$ is shown in comparison with other computed results. Two numerical results with different grid sizes are shown from the present computations. Both results, 21×21 and 31×31, are in good agreement with those of Burggraf [14] and Goda [15]. Although not shown here, Goda reported a rather poor agreement when he used a 21×21 mesh for this Reynolds number. In Table II, the magnitudes of the stream-function and vorticity at the center of the primary vortex from the present calculations are compared with those of the other investigators [16-18] at Re = 1000. In Table III, for different Reynolds numbers, the same quantities from the vorticity stream-function calculations of Ghia et al. [16] and Schreiber and Keller [18] are compared.

In their experimental study, Koseff et al. [19] observed Taylor-Gortler type vortices, which are formed as a result of the streamline curvature owing to the primary vortex. This is the first observation of such vortices in a cavity flow. Their numerical simulation, however, failed to reproduce this three-dimensional structure. To initialize the calculation in the present study, small random disturbances in the spanwise direction (x_3) were added to the solution of two-dimensional cases. Using periodic boundary conditions in the spanwise direction, the computations were carried out for various Reynolds numbers. In Fig. 7, the velocity vectors in the plane perpendicular to the primary vortex show the existence of the counterrotating vortices at Re = 1000. Although Goda [15] calculated the flow in a three-dimensional cavity, no such three-dimensional structure was reported.

4.2 Flow over a Backward-Facing Step

The flow over a backward-facing step in a channel provides an excellent test case for the accuracy of numerical method because of the dependence of the reattachment length x_r on the Reynolds number. Excessive numerical smoothing in favor of stability will result in failure to predict the correct reattachment length.

The geometry and boundary conditions for this flow are shown in Fig. 8. At the inflow boundary, located at the step, a parabolic profile was prescribed. Both Neumann and Dirichlet outflow boundary conditions were used, and the two results are identical. In Fig. 9, numerical results for different Reynolds numbers are shown in comparison with the experimental and computational results of Armaly et al. [20]. The dependence of the reattachment length on Reynolds number is in good agreement with the experimental data up to about Re = 500. At Re = 600, the computed results start to deviate from the experimental values. A mesh-refinement study, as well as variation of the location of downstream boundary at this Reynolds number, showed that the difference between the experimental and computational results is not a result of numerical errors. It is most likely, as Armaly et al. [20] have pointed out, that the difference is due to the three-dimensionality of the experimental flow at this Reynolds number. In comparison with the numerical results of Armaly et al. [20] (using TEACH code), however, the present results show a much higher reattachment length.

Armaly et al. [20] reported the existence of a secondary separation bubble on the no-step wall at Re = 1000. The length of the secondary bubble at Re = 1000 was 10.4 step-heights and the length decreased for higher Reynolds numbers. Figure 10 shows the computed streamlines at Re = 600, indicating the secondary separation bubble on the no-step wall; the bubble length is 7.8 step-heights. At Re = 800, the length increased to 11.5 step-heights.

SUMMARY

A numerical method was presented for solving three-dimensional, time-dependent incompressible flows; the method is based on the fractional-step method used in conjunction with the approximate-factorization scheme. The three-dimensional Poisson equations was solved directly by a transform method, and the velocity field satisfied the continuity equation up to machine accuracy. The method is second-order accurate in both space and time. Proper boundary conditions for the intermediate (split) velocity field were derived and tested against a known solution, and laminar flows in a driven cavity and over a backward-facing step were calculated at several Reynolds numbers. The numerical results are in good agreement with experimental data and other numerical solutions.

REFERENCES

1. A. J. CHORIN, J. Comp. Phys. 2 (1967), 12.
2. J. L. STEGER AND P. KUTLER, AIAA J. 15 (1977), 581.
3. N. A. PHILLIPS, An Example of Nonlinear Computational Instability, in "The Atmosphere and Sea in Motion," Rockefeller Inst. Press, New York, 1959.
4. A. J. CHORIN, Math. Comp. 23 (1969), 341.
5. R. TEMAM, "Navier-Stokes Equations. Theory and Numerical Analysis," 2nd ed., North-Holland Pub. Co., Amsterdam, 1979.
6. R. M. BEAM AND R. F. WARMING, J. Comp. Phys. 22 (1976), 87.
7. W. R. BRILEY AND H. McDONALD, J. Comp. Phys. 24 (1977), 428.
8. F. H. HARLOW AND J. E. WELCH, Phys. Fluids 8 (1965), 2182.
9. R. J. LeVEQUE AND J. OLIGER, "Numerical Analysis Project," Manuscript NA-81-16, Computer Science Department, Stanford University, Stanford, Calif., 1981.
10. D. K. LILLY, Monthly Weather Rev. 93 (1965), 11.
11. F. W. DORR, SIAM Review 12 (2) (1970), 248.
12. A. J. CHORIN, "The Numerical Solution of the Navier-Stokes Equations for an Incompressible Fluid," AEC Research and Development Report, NYO-1480-82, New York University, 1967.
13. C. E. PEARSON, Report No. SRRC-RR-64-17, Sperry-Rand Research Center, Sudbury, Mass., 1964.
14. O. R. BURGGRAF, J. Fluid Mech. 24 (1966), 113.
15. K. GODA, J. Comp. Phys. 30 (1979), 76.
16. U. GHIA, K. N. GHIA, AND C. T. SHIN, J. Comp. Phys. 48 (1982), 387.

17. A. S. BENJAMIN AND V. E. DENNY, J. Comp. Phys. **33** (1979), 340.

18. R. SCHREIBER AND H. B. KELLER, J. Comp. Phys. **49** (1983), 310.

19. J. R. KOSEFF, R. L. STREET, P. M. GRESHO, C. D. UPSON, J. A. C. HUMPHREY, AND W.-M. TO, "Proceedings, Third International Conference on Numerical Methods in Laminar and Turbulent Flows," (C. D. Taylor, ed.), p. 564, Seattle, Washington, Aug. 8-11, 1983.

20. B. F. ARMALY, F. DURST, AND J. C. F. PEREIRA, J. Fluid Mech. **127** (1983), 473.

TABLE I

Maximum Error after 30 Steps: $\varepsilon_{max}/u_{max}$

Grid	Boundary conditions	
	$\hat{u}_i = u_i^{n+1}$	$\hat{u}_i = u_i^{n+1} + \Delta t \frac{\partial \phi^n}{\partial x_i}$
20 × 20	8.172×10^{-4}	1.085×10^{-4}
40 × 40	1.127×10^{-3}	7.678×10^{-5}

TABLE II

Stream-Function and Vorticity at Center of Primary Vortex at Re = 1,000

	Ghia et al. [16] (129 × 129)	Present (97 × 97)	Benjamin and Denny [17] (101 × 101)	Schreiber and Keller [18] (141 × 141)
ψ_c	-0.118	-0.116	-0.118	-0.116
ξ_c	-2.050	-2.026	-2.044	-2.026

TABLE III

Stream-Function and Vorticity at Center of Primary Vortices for Different Reynolds Numbers

Re	Present	Ghia *et al.* [16]	Schreiber and Keller [18]
	ψ_c (ξ_c)	ψ_c (ξ_c)	ψ_c (ξ_c)
1	-0.099 (-3.316)	---	-0.100 (-3.232)
	65 × 65		121 × 121
100	-0.103 (-3.177)	-0.103 (-3.166)	-0.103 (-3.182)
	65 × 65	129 × 129	121 × 121
400	-0.112 (-2.260)	-0.114 (-2.295)	-0.113 (-2.281)
	65 × 65	257 × 257	141 × 141
1,000	-0.116 (-2.026)	-0.118 (-2.050)	-0.116 (-2.026)
	97 × 97	129 × 129	141 × 141
3,200	-0.115 (-1.901)	-0.120 (-1.989)	---
	97 × 97	129 × 129	
4,000	-0.114 (-1.879)	---	-0.112 (-1.805)
	97 × 97		161 × 161
5,000	-0.112 (-1.812)	-0.119 (-1.860)	---
	97 × 97	257 × 257	

Figure Captions

FIG. 1. The staggered mesh in two dimensions.

FIG. 2. Maximum error as a function of mesh refinement.

FIG. 3. Geometry of the driven cavity flow.

FIG. 4. Streamlines and contours of constant vorticity. (a) Re = 1; (b) Re = 400; (c) Re = 2,000.

FIG. 5. Velocity vectors. (a) Re = 1; (b) Re = 100; (c) Re = 400; (d) Re = 1,000; (e) Re = 2,000; (f) Re = 5,000.

FIG. 6. Profile of streamwise velocity at the midplane of the cavity (x_1 = 0.5L) for Re = 400.

FIG. 7. Velocity vectors in an (x_2 - x_3) plane through the geometric center of the cubic cavity.

FIG. 8. Flow over a backward-facing step (1:2 expansion ratio).

FIG. 9. Reattachment length as a function of Reynolds number.

FIG. 10. Streamlines at Re = 600.

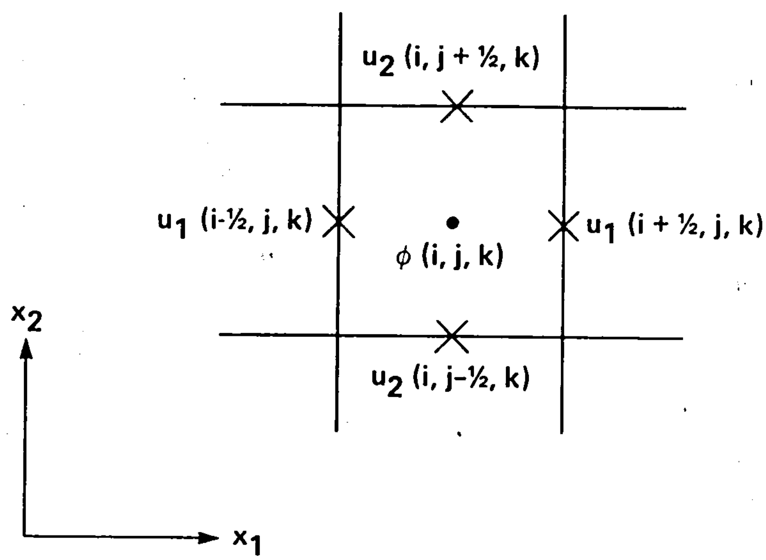

Fig. 1

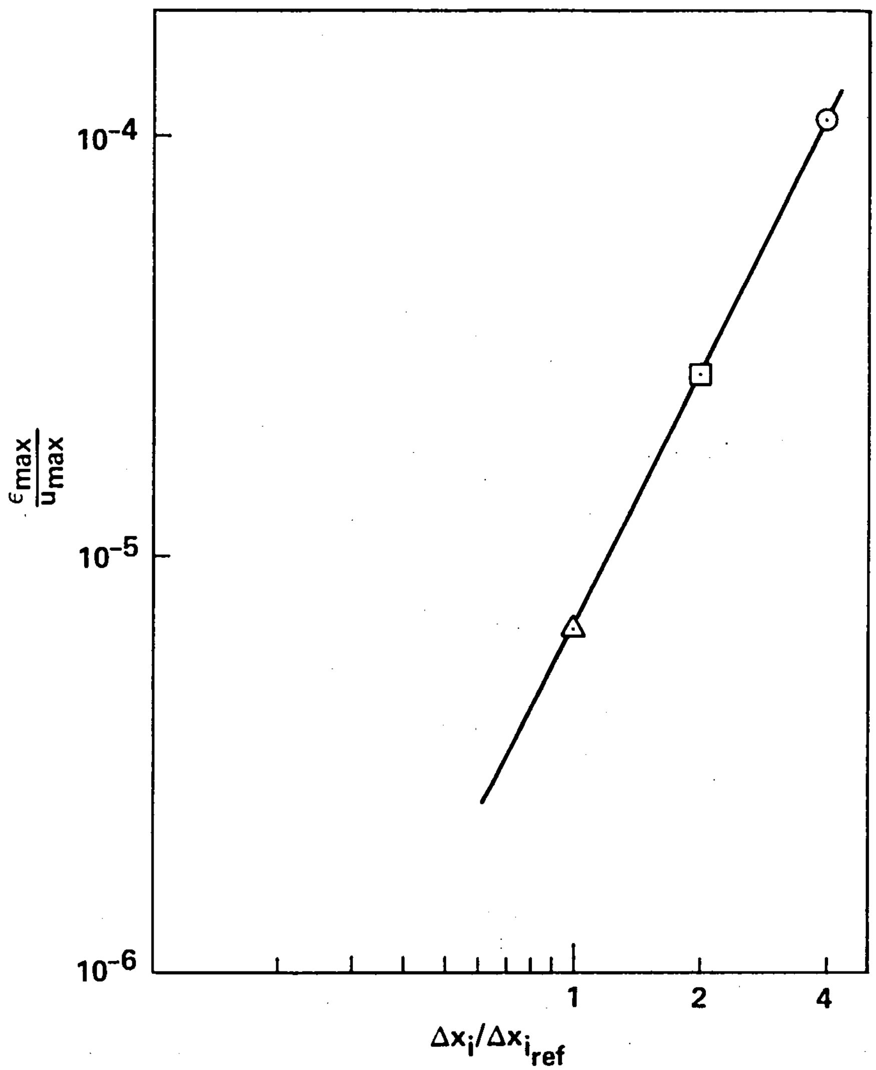

Fig. 2

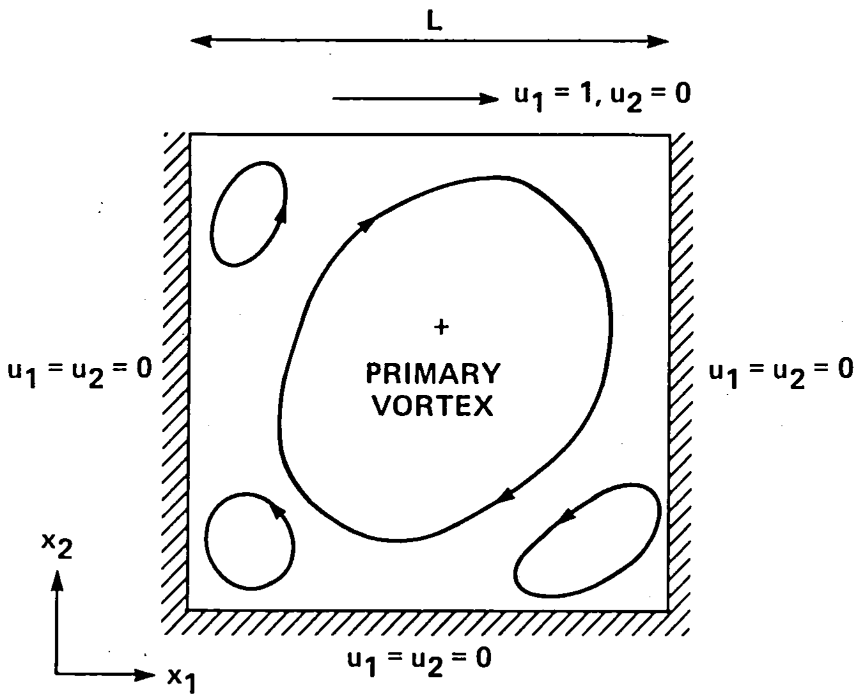

Fig. 3

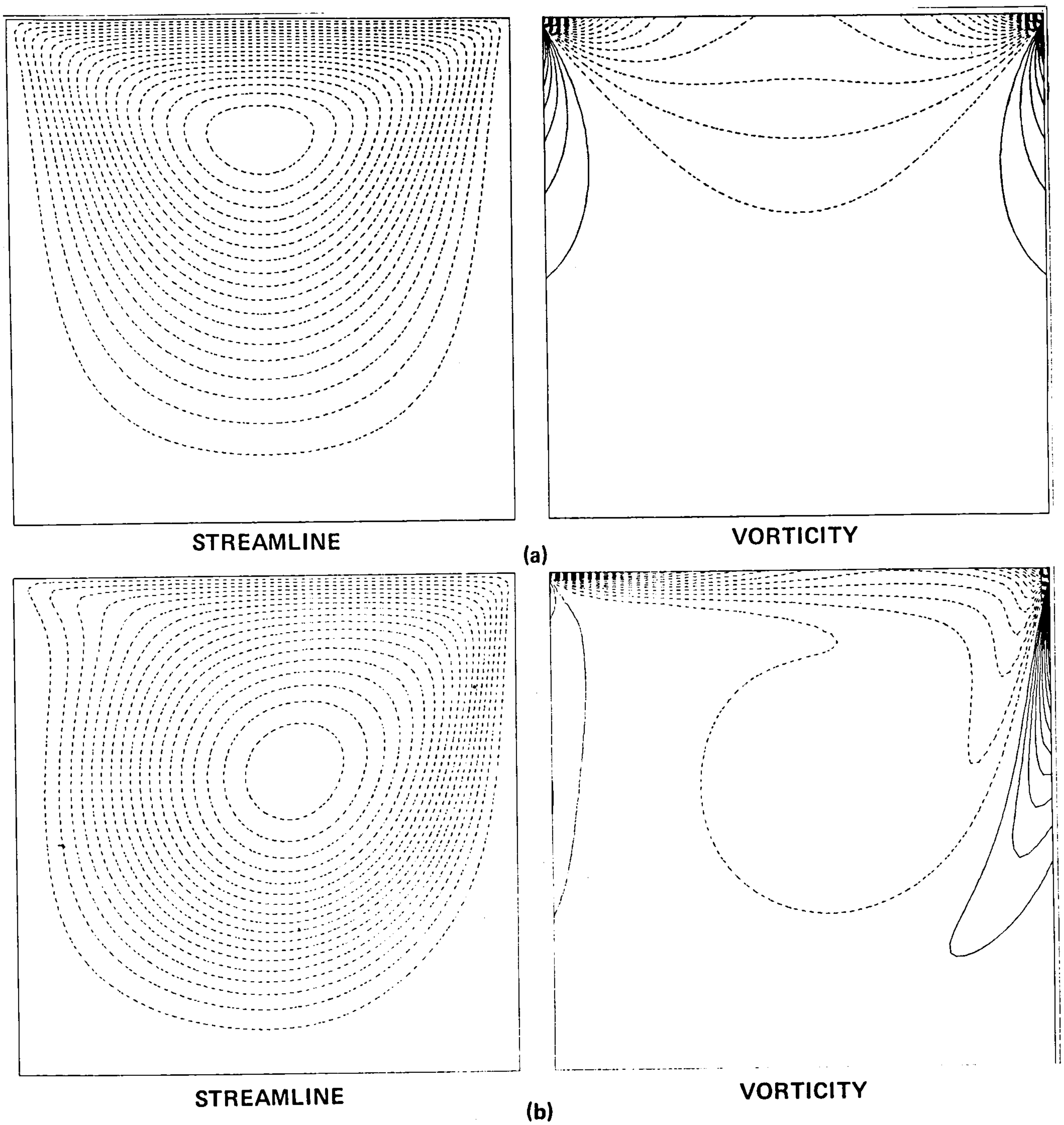

Fig. 4 (a-b)

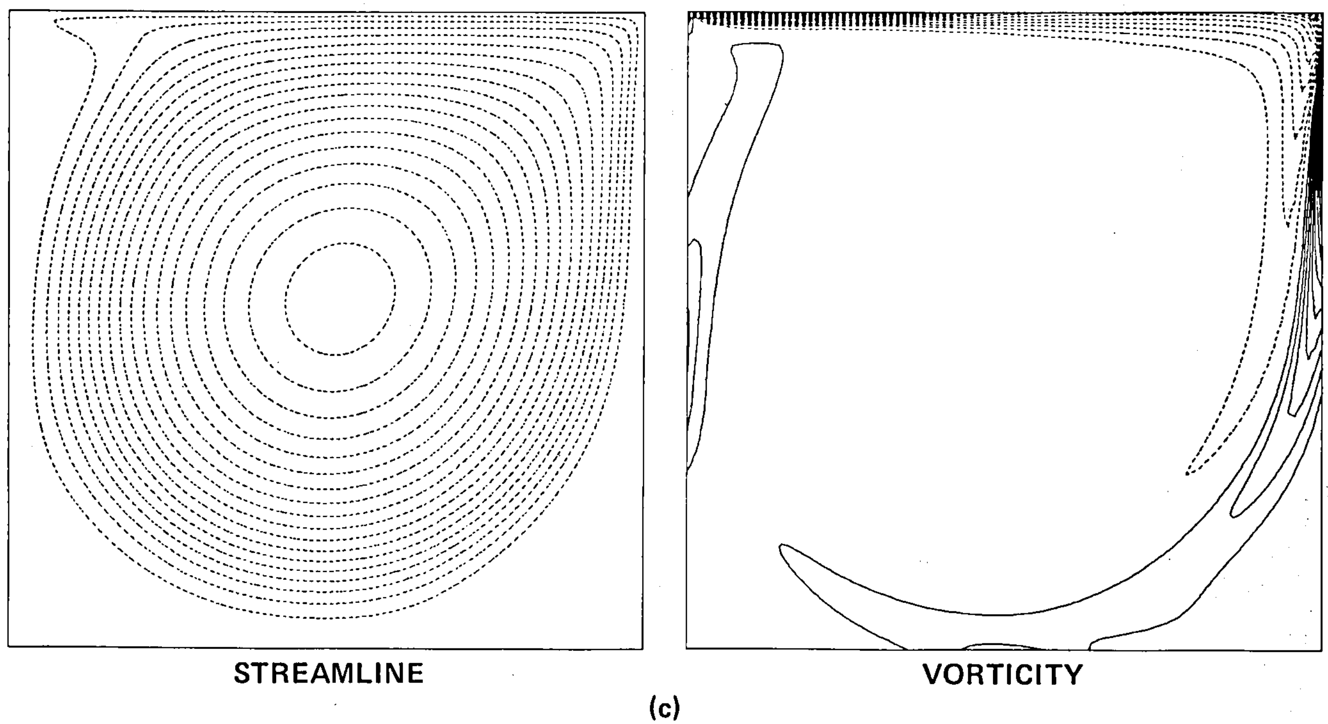

Fig. 4 (c)

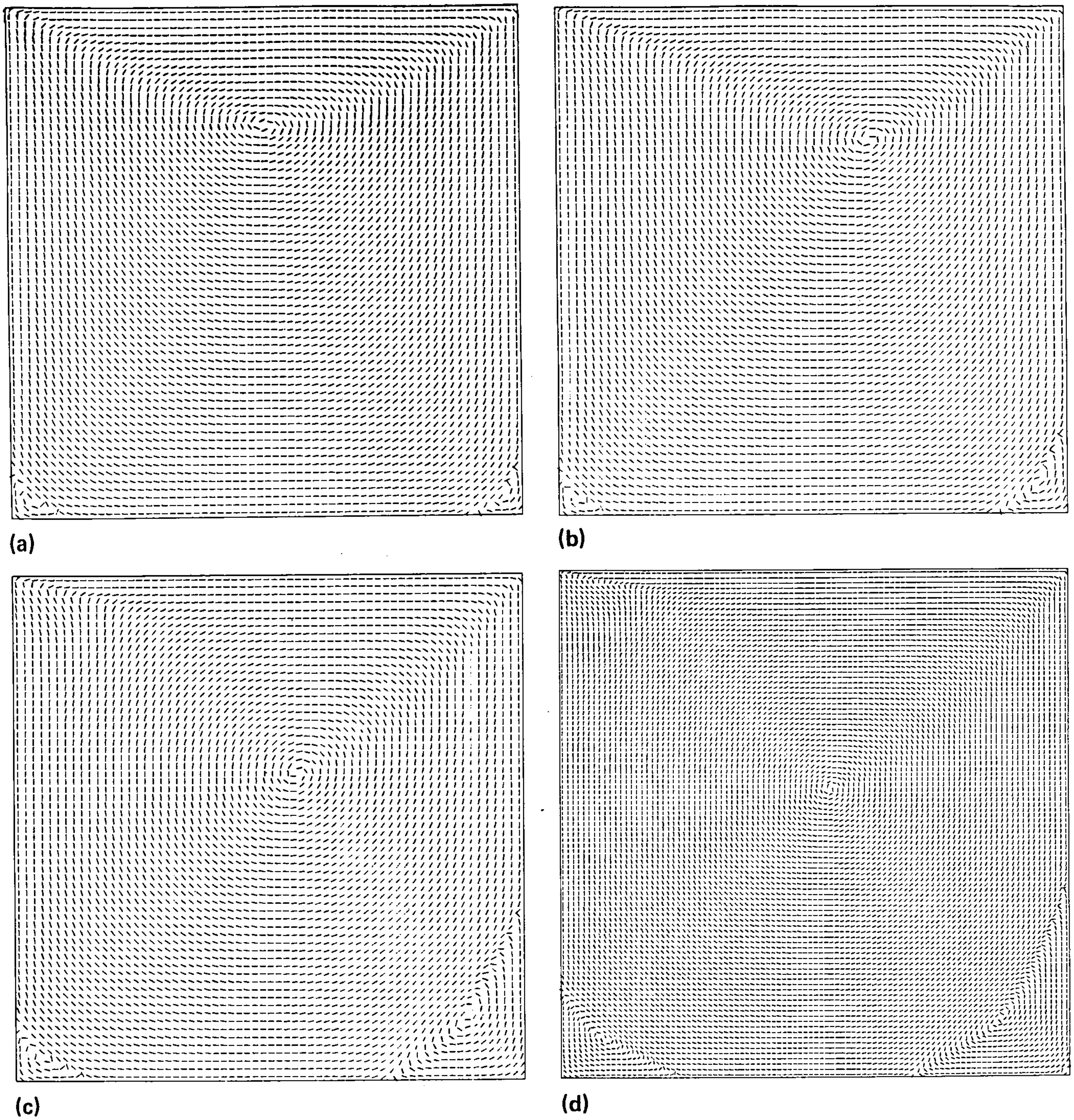

Fig. 5 (a-d)

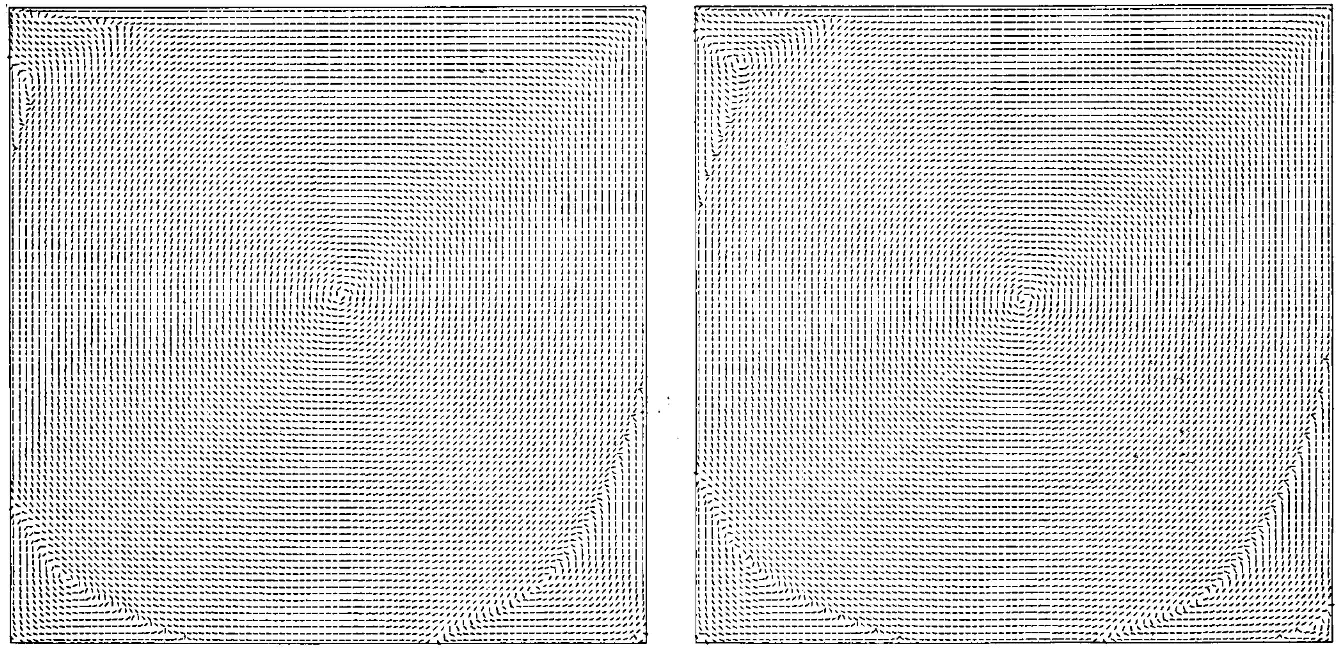

(e) (f)

Fig. 5 (e)(f)

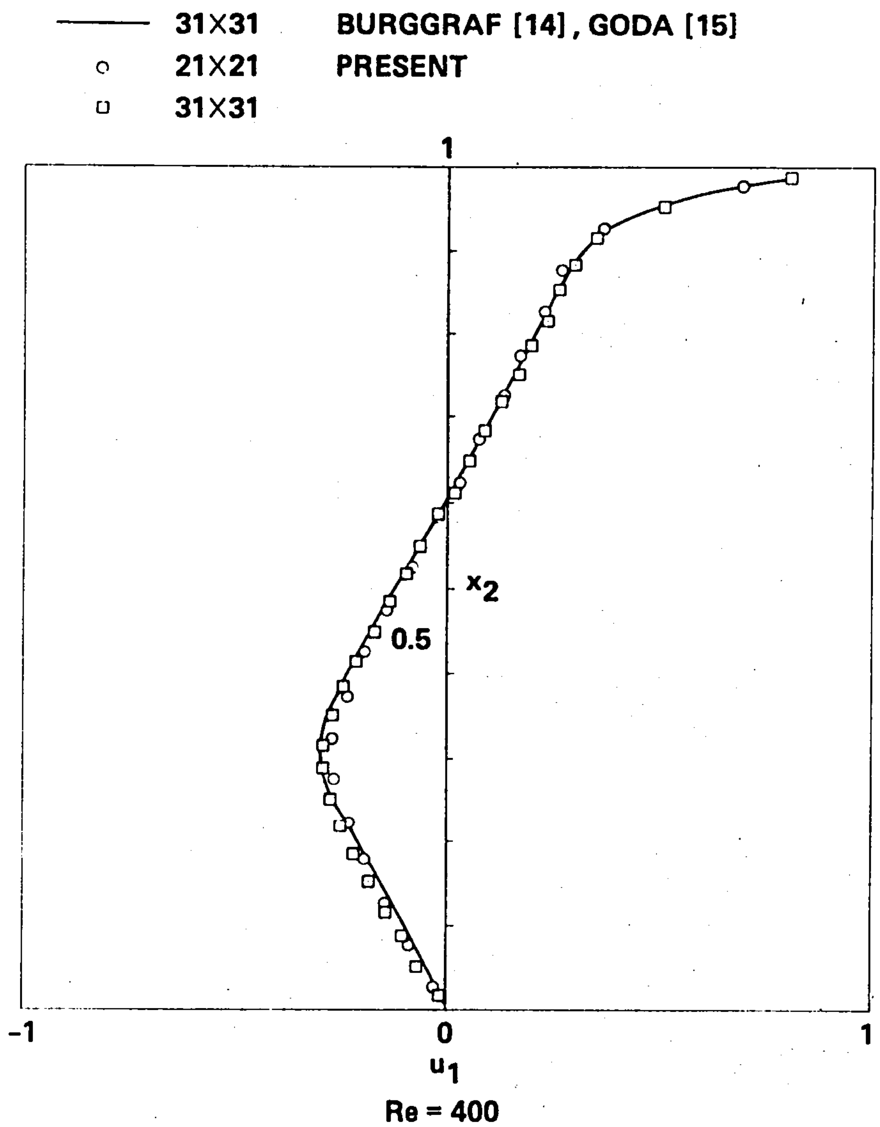

31X31 BURGGRAF [14], GODA [15]
21X21 PRESENT
31X31
1
0.5
x2
-1
0
1
u1
Re = 400

Fig. 6

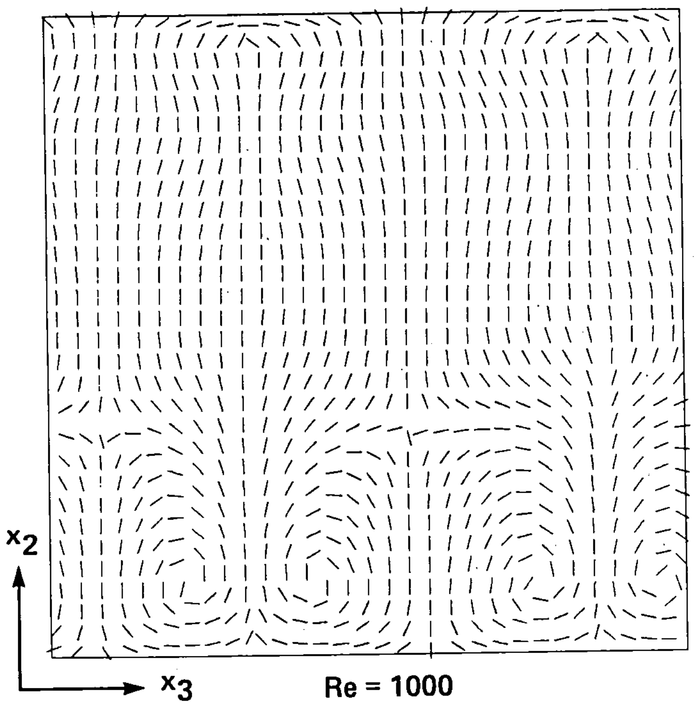

Fig. 7

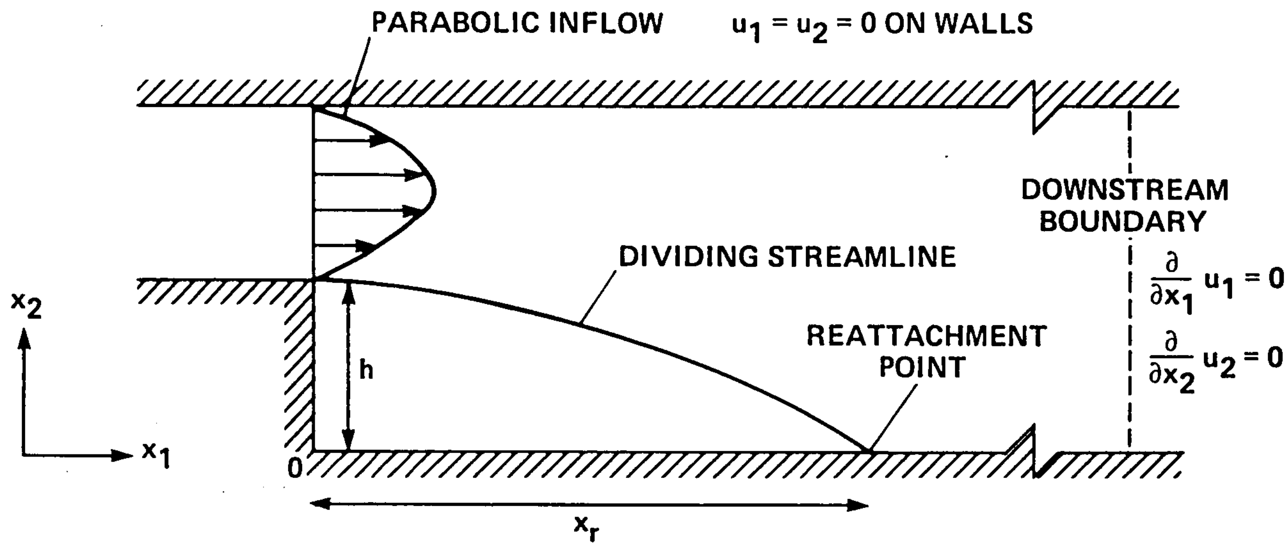
PARABOLIC INFLOW
$u_1 = u_2 = 0$ ON WALLS
DOWNSTREAM BOUNDARY
DIVIDING STREAMLINE
$\frac{\partial}{\partial x_1} u_1 = 0$
$\frac{\partial}{\partial x_2} u_2 = 0$
REATTACHMENT POINT
x_2
x_1
h
0
x_r

Fig. 8

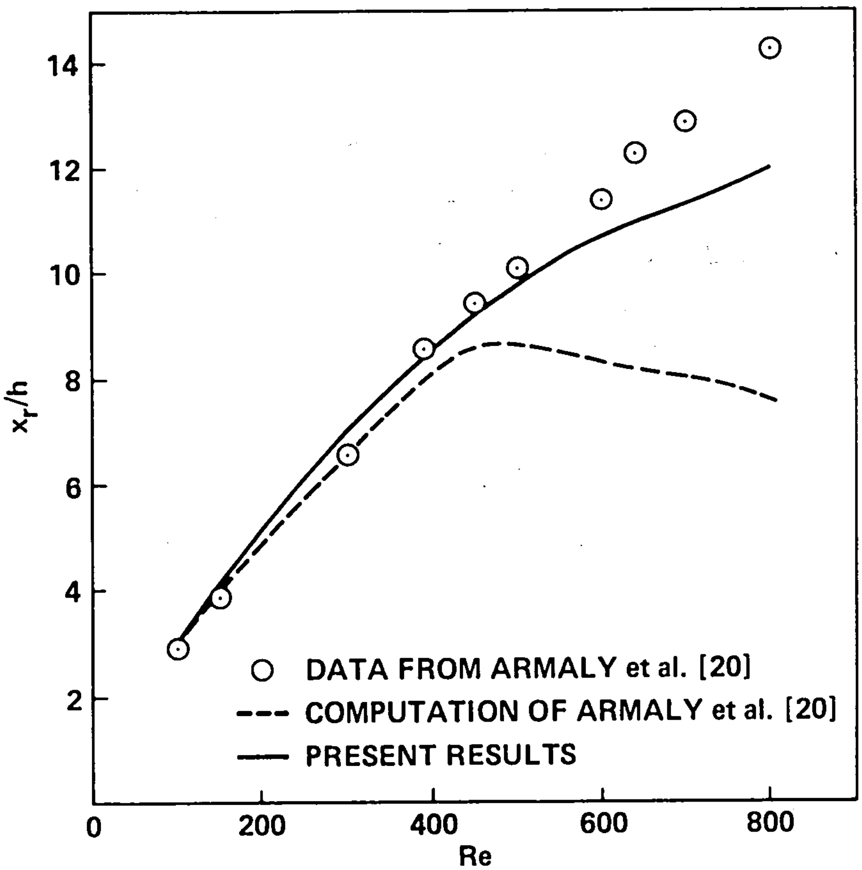

14
12
10
8
6
4
2
x_r/h
0
200
400
600
800
Re
DATA FROM ARMALY et al. [20]
COMPUTATION OF ARMALY et al. [20]
PRESENT RESULTS

Fig. 9

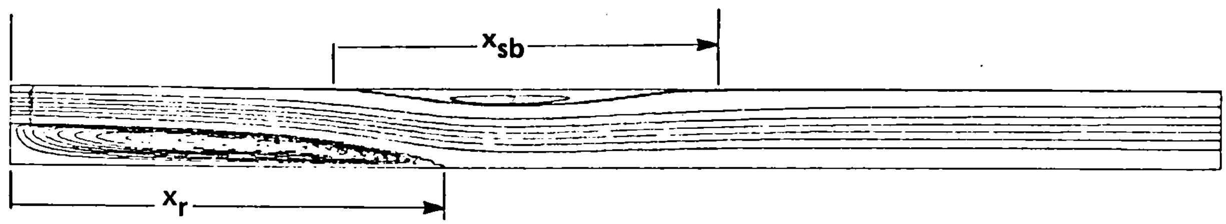

Fig. 10

1. Report No. NASA TM-85898	2. Government Accession No.	3. Recipient's Catalog No.
4. Title and Subtitle APPLICATION OF A FRACTIONAL-STEP METHOD TO INCOMPRESSIBLE NAVIER-STOKES EQUATIONS		5. Report Date March 1984
		6. Performing Organization Code ATP
7. Author(s) J. Kim and P. Moin		8. Performing Organization Report No. A-9665
		10. Work Unit No. T-6465
9. Performing Organization Name and Address Ames Research Center Moffett Field, CA 94035		11. Contract or Grant No.
		13. Type of Report and Period Covered Technical Memorandum
12. Sponsoring Agency Name and Address National Aeronautics and Space Administration Washington, DC 20546		14. Sponsoring Agency Code 505-31-01-01

15. Supplementary Notes

Point of Contact: J. Kim, Ames Research Center, MS 292A-1, Moffett Field, CA 94035 (415) 965-5576 or FTS 448-5576

16. Abstract

A numerical method for computing three-dimensional, time-dependent incompressible flows is presented. The method is based on a fractional-step, or time-splitting, scheme in conjunction with the approximate-factorization technique. It is shown that the use of velocity boundary conditions for the intermediate velocity field can lead to inconsistent numerical solutions. Appropriate boundary conditions for the intermediate velocity field are derived and tested. Numerical solutions for flows inside a driven cavity and over a backward-facing step are presented and compared with experimental data and other numerical results.

17. Key Words (Suggested by Author(s))	18. Distribution Statement
Numerical method Navier-Stokes equations Fractional-step methods	Unlimited Subject category: 64

19. Security Classif. (of this report)	20. Security Classif. (of this page)	21. No. of Pages	22. Price*
Unclassified	Unclassified	35	A03

*For sale by the National Technical Information Service, Springfield, Virginia 22161